IEEE Access
Multidisciplinary | Rapid Review | Open Access Journal

Received June 1, 2020, accepted June 7, 2020, date of publication June 10, 2020, date of current version June 24, 2020.

Digital Object Identifier 10.1109/ACCESS.2020.3001293

Simultaneous Time-Delay and Data-Loss Compensation for Networked Control Systems With Energy-Efficient Network Interfaces

TAKAHARU YAMANAKA, KENTA YAMADA, RYOSUKE HOTCHI, AND RYOGO KUBO, (Member, IEEE)

Department of Electronics and Electrical Engineering, Keio University, Yokohama 223-8522, Japan

Corresponding author: Takaharu Yamanaka (yamanaka.takaharu@kbl.elec.keio.ac.jp)

This work was supported in part by the JSPS KAKENHI under Grant 18K11275.

ABSTRACT Networked control systems (NCSs), in which controllers and actuators are connected by communication networks, have been utilized in both industrial and consumer applications. In addition, sleep-based energy-efficient network interfaces have been developed for constructing a green networked society. The combination of the NCSs and energy-efficient network interfaces is a promising approach to reduce the power consumption of NCSs. However, sleeping of the network interface results in loss of data to be transmitted between a controller and an actuator. The sleep-induced data loss causes degradation of control performance. Moreover, NCSs originally include network delay for both forward and feedback paths, which also degrades control performance. This paper proposes a time-delay and data-loss compensation method using a modified communication disturbance observer (MCDOB) for NCSs with sleep-based energy-efficient interfaces. The proposed MCDOB can simultaneously compensate for not only the network delay but also sleep-induced data loss as a disturbance, whereas a conventional communication disturbance observer (CDOB) considers only network delay or network-induced data loss and cannot be directly introduced into the NCSs with sleep-based energy-efficient interfaces. Experimental results show that the proposed method with MCDOB outperforms the conventional method without the MCDOB in terms of integral square error (ISE) and communication rate, which indicates the power consumption of network interfaces.

INDEX TERMS Communication disturbance observer, data loss, energy-efficient network, networked control system, time delay.

I. INTRODUCTION

Recently, remarkable developments have been made in information and communication technology (ICT). For example, based on its ability to connect various devices to the Internet, Internet of things (IoT) is gaining broad popularity [1]. This technology allows us to remotely control devices and measure their states. One of the basic technologies employed is networked control systems (NCSs) [2]–[4]. In NCSs, controllers are connected to sensors and actuators via the Internet and remote entities can be controlled. This system is used in various areas, such as unmanned aerial vehicles [5], remote surgery [6], and distributed power generation networks [7] because of its advantages such as low cost and great flexibility. However, the network traffic between controllers and sensors/actuators is increasing with the increased use of NCSs, which also causes an increase in the power consumption of network interfaces. Reducing the network traffic in NCSs and power consumption of network interfaces is an important issue.

Various approaches to reduce the network traffic in NCSs have been proposed. Farjam *et al.* [8] proposed a timer-based distributed channel access mechanism for NCSs including multiple different control subsystems to effectively allocate the limited communication resource to each subsystem. Rahnama *et al.* [9] proposed the passivity-based design method for NCSs to realize finite-gain L_2-stability of event-triggered NCSs. Batmani *et al.* [10] proposed the event-triggered method based on the state-dependent Riccati equation (SDRE) approach to reduce the communication

The associate editor coordinating the review of this manuscript and approving it for publication was Nasim Ullah.

rate between the SDRE controller and actuator in various classes of nonlinear discrete-time NCSs. However, the above-mentioned methods focus on only the reduction of network traffic in NCSs, and the energy-efficient operation of their network interfaces have not been considered.

Nowadays, sleep-based energy-efficient network interfaces have been developed for developing a green networked society. Sleep-based energy-efficient network interfaces have been proposed for various network systems such as the Energy Efficient Ethernet (EEE) [11]–[13] and sleep modes for passive optical networks (PONs) [14]–[16]. The power consumption can be reduced by entering a sleep period when there is little traffic. In the EEE, transceivers are assumed to take several microseconds to wake up. In contrast, in PONs, the sleep period should be much longer to reduce the power consumption effectively because optical transceivers need a longer time to wake up [17]. However, in NCSs, the control performance can be degraded if the sleep period is long. Therefore, building the NCSs using energy-efficient network interfaces which need more than several milliseconds to wake up is a challenging task.

Iino *et al.* [18] proposed a novel concept of event-predictive control to reduce the power consumption of wireless network nodes in NCSs, which extended event-triggered control used for traffic reduction. A sleep control method of optical transceivers for NCSs has been also discussed. In [19], the controller determined when the network interfaces enter the sleep period by comparing the latest and previously transmitted data. However, the NCS with sleep-based energy-efficient network interfaces generated loss of data to be transmitted between a controller and an actuator. The sleep-induced data loss causes the degradation of control performance, and its compensation method has not been clarified.

In general NCSs without energy-efficient network interfaces, the control performance is degraded by network-induced delay and data loss for both forward and feedback paths [20]. Various approaches have been proposed to compensate for the network-induced delay, such as sliding mode control [21], optimal control [22], and model predictive control [23]. As delay compensators, the Smith predictor [24], adaptive Smith predictor [25]–[27], and communication disturbance observer (CDOB) [28]–[30] have been used in many previous studies. The Smith predictor can be used only for a fixed network delay, whereas the adaptive Smith predictor can compensate for a time-varying network delay by measuring the round-trip time (RTT) and updating the delay model. However, these Smith predictors cannot compensate for network-induced data loss. In contrast, the CDOB can compensate for both the time-varying network delay and network-induced data loss [31]. There have been also other approaches to compensate for network-induced data loss, such as model-based predictive control [32], estimation of distribution algorithm (EDA) [33], and H_∞ control [34]. However, these approaches cannot deal with the sleep-induced data loss because they consider only network-induced delay and data loss in NCSs without energy-efficient network interfaces.

This research considers the NCS with sleep-based energy-efficient network interfaces proposed in [19] as a basic system configuration. The conventional system did not have any compensation scheme for the sleep-induced data loss. This paper proposes a time-delay and data-loss compensation method using a modified communication disturbance observer (MCDOB) for the NCSs with energy-efficient network interfaces. The MCDOB can simultaneously compensate for not only the network delay but also sleep-induced data loss as a disturbance. Though the MCDOB was inspired by the CDOB, the novelty lies in modeling of the disturbance and modified implementation into the NCS by taking the sleep-induced data loss into account. The feature of the NCS with sleep-based energy-efficient network interfaces is that the sleep-induced data loss on the forward path can be precisely recognized by the controller. By taking advantage of this feature, in the MCDOB, we remove the effect of sleep-induced data loss only on the forward path from the disturbance model while the CDOB cannot separate the disturbance into forward and feedback parts. Experimental results show that the proposed method with the MCDOB outperforms the conventional method without the MCDOB in terms of integral square error (ISE) and communication rate, which indicates power consumption. We showed the basic concept of the MCDOB and its preliminary results in [35]. This paper further discusses the introduction of energy-efficient network interfaces, their modeling, and additional experimental validation.

This paper is organized as follows: The following section describes the NCS for robust motion control. Section III describes a basic configuration of the NCS with energy-efficient network interfaces. Section IV describes the proposed time-delay and data-loss compensation using the MCDOB. Section V shows experimental results. Finally, our conclusion is described in section VI.

II. NCS

This section describes the networked motion control system including the disturbance observer (DOB) for robust motor control and CDOB for network delay compensation. This research focuses on the networked motion control system as an NCS.

A. NETWORKED MOTION CONTROL

The networked angle control system of a direct current (DC) motor is shown in Fig. 1. In Fig. 1, θ^{cmd}, u, θ^{res}, and $\dot{\theta}^{res}$ are the angle command, control input, angle response, and angular velocity response, respectively. This system includes a proportional-derivative (PD) controller G_c and the nominal model of the DC motor, P_n, which is represented as (1)

$$P_n = \frac{K_n}{\tau_n s}, \tag{1}$$

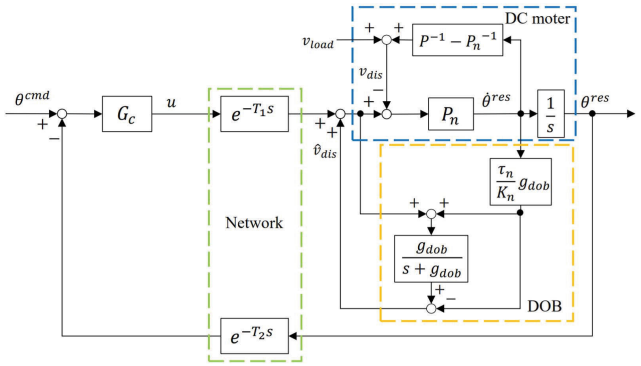

FIGURE 1. Networked angle control system of a DC motor.

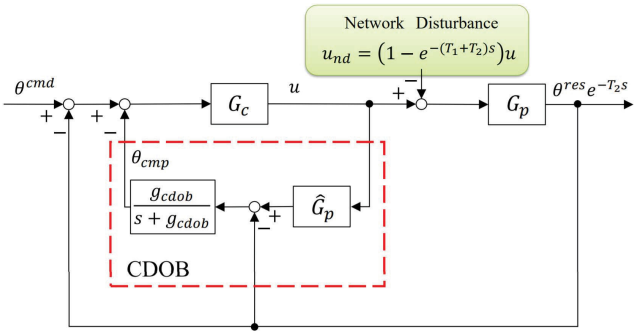

FIGURE 2. Networked angle control system with CDOB.

where s, K_n, and τ_n denote the Laplace operator, nominal steady-state gain of the motor, and nominal time constant of the motor, respectively. In the NCS, there are transmission delays for the forward path T_1 and the feedback path T_2. In this research, the transmission delays are modeled as a constant value because we assume that the delays can be kept at a constant level by using a jitter buffer to absorb delay variations [36]. The transmission delays are both longer than a control period t_c and set to a multiple of t_c. The delay shorter than a control period t_c is treated as a sampling delay. In addition, the NCS does not include the network-induced data loss because we assume that a wired and bandwidth-guaranteed communication network is utilized. It is true that cybersecurity issues are very important in building NCSs, but their impact is mitigated by using secure and reliable communication networks such as a virtual private network (VPN) in this research.

An actual motor may include disturbances such as the load torque and modeling error of the motor. The disturbance, v_{dis}, can be expressed as (2)

$$v_{dis} = v_{load} + (P^{-1} - P_n^{-1})\dot{\theta}^{res}, \tag{2}$$

where v_{load} and P denote the effect of the load torque and transfer function of the actual DC motor, respectively. The motor dynamics P is expressed as (3)

$$P = \frac{K}{\tau s + 1}, \tag{3}$$

where K and τ denote the actual steady-state gain of the motor and time constant of the motor, respectively. To compensate for the disturbance, v_{dis}, the DOB [37] is used as shown in Fig. 1. The disturbance estimated by the DOB, $\hat{v}_{dis}$, can be expressed as (4)

$$\hat{v}_{dis} = \frac{g_{dob}}{s + g_{dob}} v_{dis}, \tag{4}$$

where g_{dob} denotes the cut-off frequency of the DOB. If g_{dob} is sufficiently large, the DOB can completely suppress the disturbance, and robust control can be achieved.

B. CDOB

The CDOB estimates the time-delay effect on the system as a network disturbance and compensates for it [28]. Figure 2 shows the networked motion control system using CDOB. In Fig. 2, G_p, u_{nd}, and θ_{cmp} are the transfer function of a motor system including the DOB, network disturbance, and compensation value, respectively. The transfer function of a motor system including the DOB, G_p, is ideally expressed as (5)

$$G_p = \frac{P_n}{s}. \tag{5}$$

The network delays are considered as the network disturbance, u_{nd}, expressed as (6)

$$u_{nd} = (1 - e^{-(T_1+T_2)s})u. \tag{6}$$

The compensation value, θ_{cmp}, is calculated as (7)

$$\theta_{cmp} = \frac{g_{cdob}}{s + g_{cdob}}(\hat{G}_p u - \theta^{res} e^{-T_2 s}), \tag{7}$$

where $\hat{G}_p$ and g_{cdob} are the nominal model of the motor system including the DOB and cut-off frequency of the CDOB, respectively. When the cut-off frequency of the DOB is sufficiently large and $\hat{G}_p$ is equal to G_p, (7) can be transformed into (8)

$$\theta_{cmp} = \frac{g_{cdob}}{s + g_{cdob}} G_p u_{nd}. \tag{8}$$

When the cut-off frequency of the CDOB is sufficiently large, the transfer function from θ^{cmd} to θ^{res}, T_{cmp}, is calculated as (9)

$$T_{cmp} = \frac{G_c G_p e^{-T_1 s}}{1 + G_c G_p}. \tag{9}$$

In contrast, when the CDOB is not implemented, the transfer function from θ^{cmd} to θ^{res}, T_{nocmp}, is calculated as (10)

$$T_{nocmp} = \frac{G_c G_p e^{-T_1 s}}{1 + G_c G_p e^{-(T_1+T_2)s}}. \tag{10}$$

In (9), the network delay can be eliminated from the denominator of the transfer function differently from (10), which means that the controller can be designed without considering the effect of network delay with respect to

closed-loop stability. The relationship between the network disturbance and stability has been discussed in [38]–[40]. The cut-off frequencies of the CDOB and DOB affect the compensation performance of the network disturbance, including various constraints such as upper bound of time delay.

III. NCS WITH ENERGY-EFFICIENT NETWORK INTERFACES

This section describes the system configuration of a sleep-based energy-efficient NCS and its sleep mechanisms to reduce the power consumption of network interfaces.

A. SYSTEM CONFIGURATION

Figure 3 shows the operation of a sleep-based energy-efficient transmitter. In Fig. 3, T_{active} and T_{sleep} are the periods during which the transmitter is in active mode and sleep mode, respectively. The power consumption of the transmitter in the active mode, P_{active}, is generally larger than that in the sleep mode, P_{sleep}. The power consumption of the network interface can be reduced by the transmitter repeatedly entering the sleep mode and returning from the sleep mode to active mode. While the transmitter is in the sleep mode, it is powered off and stops transmitting data.

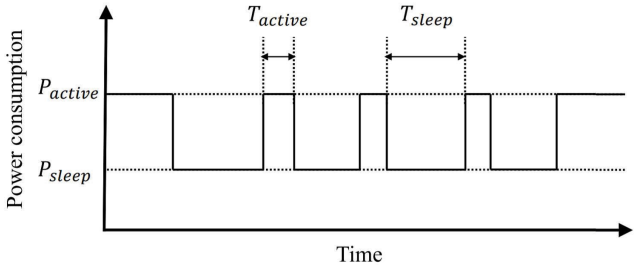

FIGURE 3. Operation of a sleep-based energy-efficient transmitter.

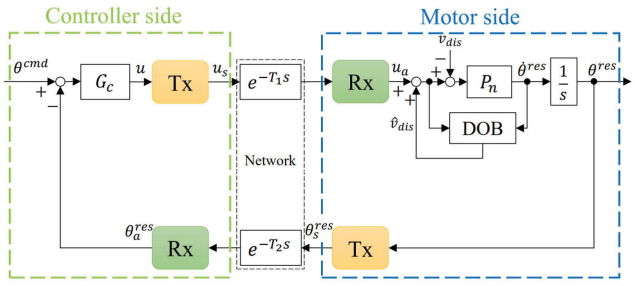

FIGURE 4. Energy-efficient NCS.

Figure 4 shows the system configuration of the NCS with the sleep-based energy-efficient network interfaces for forward and feedback paths. In Fig. 4, u_s, u_a, θ_s^{res}, and θ_a^{res} are the control input transmitted from the controller side, control input used in the motor side, angle response transmitted from the motor side, and angle response used in the controller side, respectively.

In the energy-efficient NCS, the communication frequencies decrease on the forward and feedback paths, i.e., the path

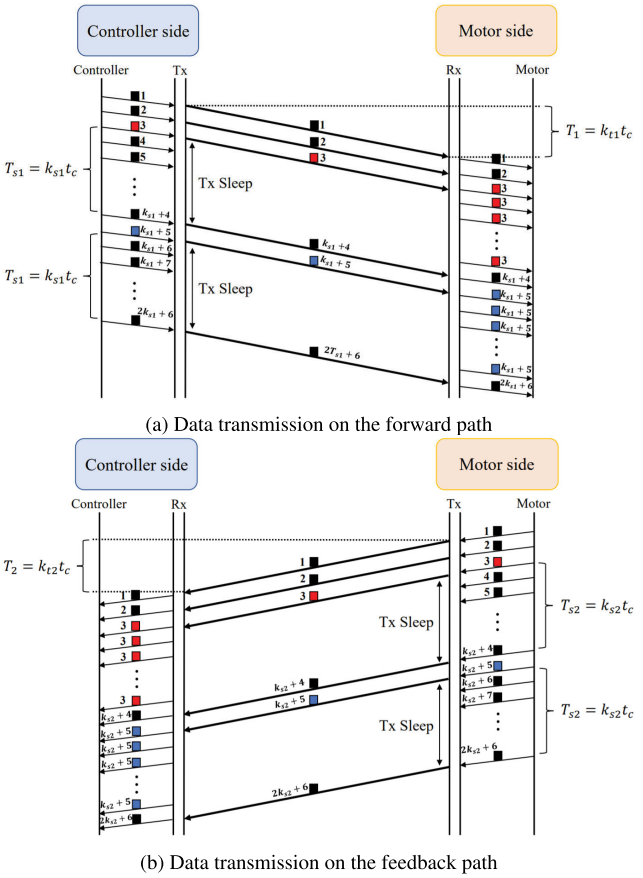

(a) Data transmission on the forward path

(b) Data transmission on the feedback path

FIGURE 5. Communication between controller side and motor side.

from the controller to motor sides and the path from motor to controller sides, as shown in Fig. 5. In Fig. 5, T_{s1} and T_{s2} are the sleep periods for the transmitters on the controller and motor sides, respectively. The sleep periods, T_{s1} and T_{s2}, are expressed as $T_{s1} = k_{s1}t_c$ and $T_{s2} = k_{s2}t_c$, where k_{s1}, k_{s2}, and t_c denote the numbers of samples during T_{s1} and T_{s2} and control period, respectively. The network delays, T_1 and T_2, are expressed as $T_1 = k_{t1}t_c$ and $T_2 = k_{t2}t_c$, where k_{t1} and k_{t2} denote the numbers of samples during T_1 and T_2, respectively. On the controller side, when the transmitter is shifted to the sleep mode, the transmitter is powered off and stops transmitting data during T_{s1}. Similarly, on the motor side, when the transmitter is shifted to the sleep mode, the transmitter is powered off and stops transmitting data during T_{s2}. While each transmitter is in the sleep mode, the corresponding receiver utilizes the latest data received in the previous sampling times because it cannot receive data from the transmitter.

B. SLEEP MECHANISMS OF NETWORK INTERFACES

Algorithms 1 and 2 show the operation of the transmitter on the controller side and operation of the receiver on the motor side, respectively. In Algorithm 1, S_c, h_1, k, k_{end}, and k_0 denote the state of the transmitter on the controller side, voltage threshold for the forward path, sampling time, ending

Algorithm 1 Operation of the Transmitter on the Controller Side

$S_c \Leftarrow 1$
for $k \Leftarrow 0$ to k_{end} **do**
  if $S_c = 1$ **then**
    if $|u(k) - u_s(k-1)| < h_1$ **then**
      $k_0 \Leftarrow k$
      $S_c \Leftarrow 0$
    end if
  else if $k \geq k_0 + k_{s1}$ **then**
    $S_c \Leftarrow 1$
  end if
end for

Algorithm 2 Operation of the Receiver on the Motor Side

for $k \Leftarrow 0$ to k_{end} **do**
  if the Rx received no new data from the Tx **then**
    $u_a(k) \Leftarrow u_a(k-1)$
  else
    $u_a(k) \Leftarrow u_s(k - k_{t1})$
  end if
end for

Algorithm 3 Operation of the Transmitter on the Motor Side

$S_m \Leftarrow 1$
for $k \Leftarrow 0$ to k_{end} **do**
  if $S_m = 1$ **then**
    if $|\theta^{res}(k) - \theta_s^{res}(k-1)| < h_2$ **then**
      $k_0 \Leftarrow k$
      $S_m \Leftarrow 0$
    end if
  else if $k \geq k_0 + k_{s2}$ **then**
    $S_m \Leftarrow 1$
  end if
end for

Algorithm 4 Operation of the Receiver on the Controller Side

for $k \Leftarrow 0$ to k_{end} **do**
  if the Rx received no new data from the Tx **then**
    $\theta_a^{res}(k) \Leftarrow \theta_a^{res}(k-1)$
  else
    $\theta_a^{res}(k) \Leftarrow \theta_s^{res}(k - k_{t2})$
  end if
end for

sampling time, and beginning sampling time for the sleep mode, respectively. The state, S_c, is set to 1 when the transmitter is in the active mode, while S_c is set to 0 when it is in the sleep mode. The transmitter on the controller side compares the variation between the latest data from the controller, $u(k)$, and the latest data transmitted to the motor side, $u_s(k-1)$, with the threshold, h_1, when the transmitter is in active mode. If the variation is smaller than h_1, the transmitter is powered off and is shifted to the sleep mode during the sleep period, T_{s1}. After the sleep period, the transmitter is powered on, transmits data, and compares the variation again. In Algorithm 2, if the receiver on the motor side received no new data from the transmitter on the controller side, the receiver continues to utilize the latest data received from the corresponding transmitter as $u_a(k)$. If the receiver receives new data, the receiver uses the new data delayed because of the transmission delay for the forward path, $u_s(k - k_{t1})$, as the latest data used in the motor side, $u_a(k)$.

Algorithms 3 and 4 show the operation of the transmitter on the motor side and operation of the receiver on the controller side, respectively. In Algorithm 3, S_m and h_2 denote the state of the transmitter on the motor side and angle threshold for the feedback path, respectively. The state, S_m, is set to 1 when the transmitter is in the active mode, whereas S_m is set to 0 when it is in the sleep mode. The transmitter on the motor side compares the variation between the latest data from the encoder of the motor, $\theta^{res}(k)$, and the latest data transmitted to the controller side, $\theta_s^{res}(k-1)$, with the threshold, h_2, when the transmitter is in the active mode. If the variation is smaller than h_2, the transmitter is powered off and is shifted to the sleep mode during the sleep period, T_{s2}. After the sleep period, the transmitter is powered on, transmits data, and compares the variation again. In Algorithm 4, if the receiver on the controller side receives no new data from the transmitter on the motor side, the receiver continues to utilize the latest data received from the corresponding transmitter as $\theta_a^{res}(k)$. If the receiver receives new data, the receiver uses the new data delayed because of the transmission delay for the feedback path, $\theta_s^{res}(k - k_{t2})$, as the latest data used in the motor side, $\theta_a^{res}(k)$.

IV. TIME-DELAY AND DATA-LOSS COMPENSATION

This section describes the analytical model of the energy-efficient NCS and proposes the MCDOB to compensate for the network delay and sleep-induced data loss in the energy-efficient NCS.

A. EFFECTS OF TIME DELAY AND DATA LOSS

To analyze the energy-efficient NCS theoretically, Fig. 4 is transformed into Fig. 6. The block L_{s1} denotes the gain calculated by the forward sleep trigger (FWST) representing the operations of the transmitter and receiver on the forward path as (11)

$$L_{s1} = \begin{cases} \dfrac{u_s(k-1)}{u(k)} & \text{if } S_c = 0 \\ 1 & \text{otherwise} \end{cases}. \tag{11}$$

If the transmitter on the controller side is in the sleep mode, the receiver on the motor side uses the latest data received in the previous sampling times. Otherwise, the receiver uses the received data at the time. The block L_{s2} denotes the gain calculated by the feedback sleep trigger (FBST) representing the operations of the transmitter and receiver on the feedback

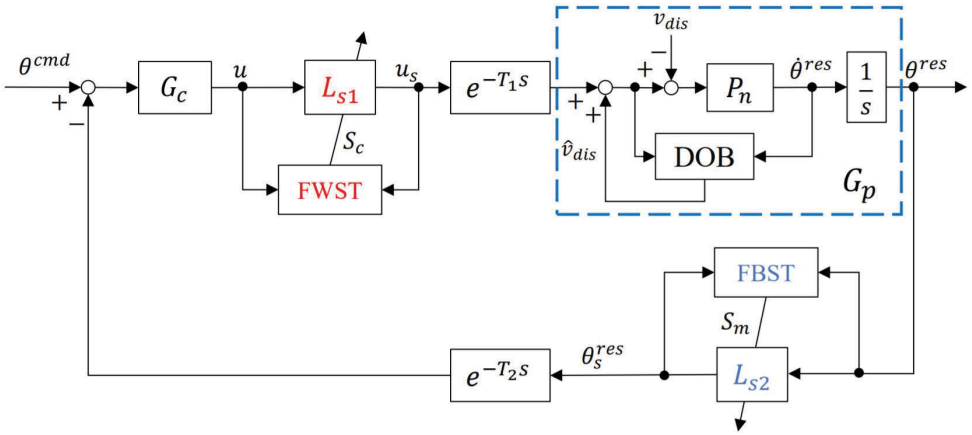

FIGURE 6. An analytical model of the energy-efficient NCS.

path as (12)

$$L_{s2} = \begin{cases} \dfrac{\theta_s^{res}(k-1)}{\theta^{res}(k)} & if\ S_m = 0 \\ 1 & otherwise \end{cases}. \tag{12}$$

If the transmitter on the motor side is in the sleep mode, the receiver on the controller side uses the latest data received in the previous sampling times. Otherwise, the receiver uses the received data at the time.

The transfer function of the controller, G_c, is expressed as (13)

$$G_c = \frac{\tau_n}{K_n}(K_p + K_d s), \tag{13}$$

where K_p and K_d denote the proportional gain and derivative gain, respectively.

The transfer function from θ^{cmd} to θ^{res}, H_{nocmp}, can be calculated as (14)

$$H_{nocmp} = \frac{G_c G_p L_{s1} e^{-T_1 s}}{1 + G_c G_p L_{s1} L_{s2} e^{-(T_1+T_2)s}}. \tag{14}$$

Notably, we assumed that the cut-off frequency of the DOB was sufficiently large. The denominator of (14) has the transfer functions of network delay and sleep-induced data loss. This means that the controller has to be designed by taking the effects of network delay and sleep-induced data loss into account.

B. COMPENSATION BY PROPOSED MCDOB

The MCDOB is proposed to compensate for the network delay and sleep-induced data loss in the energy-efficient NCS. The NCS with the MCDOB is shown in Fig. 7. The MCDOB simultaneously considers the effects of network delay and sleep-induced data loss as the disturbance, u_{us}^{dis}, shown in (15)

$$u_{us}^{dis} = (1 - L_{s2} e^{-(T_1+T_2)s}) u_s. \tag{15}$$

The disturbance includes the effects of transmission delays on both of the forward and feedback paths, i.e., T_1 and T_2, and the effects of sleep-induced data loss on only the feedback path, i.e., L_{s2}. The MCDOB does not estimate and compensate for the effects of the sleep-induced data loss on the forward path, i.e., L_{s1}, as a disturbance since the timing of the data loss, which is determined by the network interface on the controller side, can be explicitly detected on the controller.

The compensation value θ_{cmp} is calculated as (16)

$$\theta_{cmp} = \frac{g_{cdob}}{s + g_{cdob}}(\hat{G}_p u_s - \theta^{res} L_{s2} e^{-T_2 s}). \tag{16}$$

When the cut-off frequency of the DOB is sufficiently large and $\hat{G}_p$ is equal to G_p, (16) is transformed into (17)

$$\theta_{cmp} = \frac{g_{cdob}}{s + g_{cdob}} G_p u_{us}^{dis}. \tag{17}$$

When the MCDOB is implemented and its cut-off frequency, g_{cdob}, is sufficiently large, the transfer function from θ^{cmd} to θ^{res}, H_{mcdob}, can be calculated as (18)

$$H_{mcdob} = \frac{G_c G_p L_{s1} e^{-T_1 s}}{1 + G_c G_p L_{s1}}. \tag{18}$$

The transmission delays, i.e., T_1 and T_2, and sleep-induced data loss on the feedback path, i.e., L_{s2}, can be eliminated from the denominator of the transfer function, H_{mcdob}, while the sleep-induced data loss on the forward path, i.e., L_{s1}, remains in the denominator. This means that only the effect of L_{s1} has to be considered in controller design with respect to closed-loop stability.

The steady-state value of unit step response for the system with the MCDOB can be calculated as (19)

$$\lim_{t\to\infty} \theta^{res}(t) = \lim_{s\to 0} s \cdot H_{mcdob} \frac{1}{s} = 1. \tag{19}$$

From (19), there is no steady-state positional error when the MCDOB is implemented. Therefore, the MCDOB can eliminate the steady-state positional error while accepting the increase in complexity of control parameter adjustment. The controller and sleep parameters have to be designed partially by a heuristic approach. Their design strategy is shown as

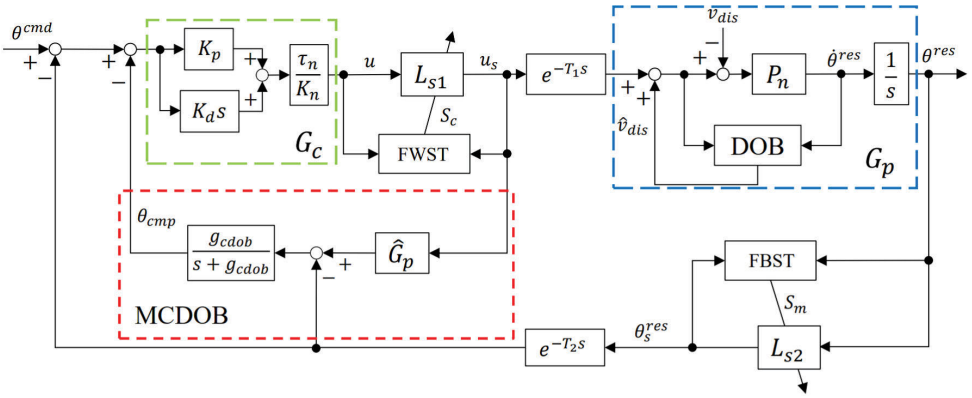

FIGURE 7. Energy-efficient NCS with the MCDOB.

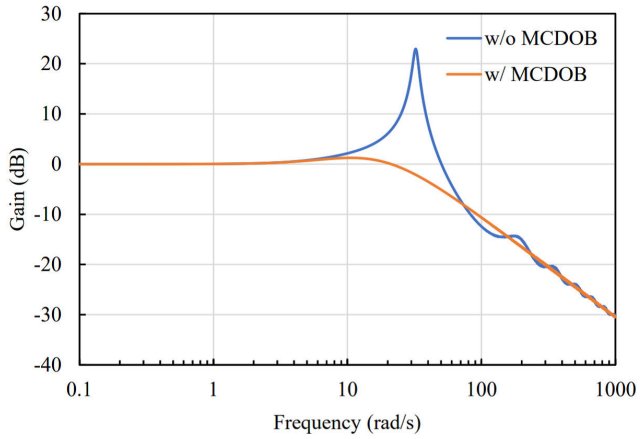

FIGURE 8. Gain characteristics of H_{nocmp} and H_{mcdob} when $L_{s1} = 1$, and $L_{s2} = 1$.

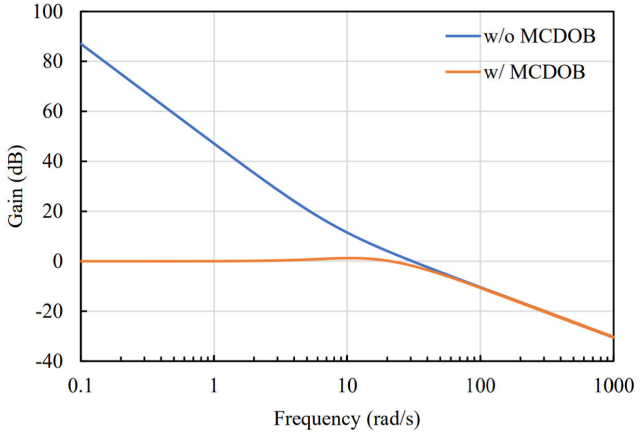

FIGURE 9. Gain characteristics of H_{nocmp} and H_{mcdob} when $L_{s1} = 1$, and $L_{s2} = 0$.

follows: First, the controller gains, K_p and K_d, are determined based on (9) within its stable region without considering L_{s1}. Then, the threshold h_2 for the feedback path is determined based on required control performance. Finally, the threshold h_1 for the forward path is determined by trial and error by considering overall stability.

The closed-loop transfer functions without MCDOB and with MCDOB, i.e., H_{nocmp} in (14) and H_{mcdob} in (18) are compared in frequency domain. The transmission delays T_1 and T_2 were both set to 20 ms. The control gains K_p and K_d were set to 225 and 30, respectively. The motor parameters K_n and τ_n were set to 1.53 and 0.0254, respectively. Figure 8 shows the gain characteristics of H_{nocmp} and H_{mcdob} when $L_{s1} = 1$ and $L_{s2} = 1$, which means no sleep-induced data loss on the forward and feedback paths. The MCDOB suppressed the peak gain at around 30 rad/s, which was caused by the transmission delays. This indicates that the MCDOB could compensate the effects of transmission delays. Figure 9 shows the gain characteristics of H_{nocmp} and H_{mcdob} when $L_{s1} = 1$ and $L_{s2} = 0$, which means no sleep-induced data loss on the forward path and an initial constant value on the feedback path. The system with MCDOB maintained the gain at 0 dB in the low-frequency range whereas the system without MCDOB increased the gain, which was caused by the sleep-induced data loss on the feedback path. This indicates that the MCDOB could compensate for the effects of sleep-induced data loss on the feedback path. The MCDOB does not compensate for the effects of the sleep-induced data loss on the forward path, L_{s1}. Therefore, we need to experimentally determine the voltage threshold h_1 by considering the required overall stability as indicated before.

In this research, the sleep-induced data loss was modeled as (11) and (12). However, there are some variations of the receiver operation when the transmitter is in the sleep mode. The MCDOB considers the transmitter and receiver operation on the feedback path as a disturbance. Therefore, the MCDOB has the potential to compensate for the effect of any receiver operation mechanisms on the feedback path. On the other hand, the MCDOB does not compensate for the effect of the transmitter and receiver operation on the forward path. Therefore, the receiver operation should be considered in designing the voltage threshold h_1. Our future works include the application of the MCDOB to the system with other transmitter and receiver operation mechanisms.

V. EXPERIMENT

This section shows the experimental results of the proposed time-delay and data-loss compensation method for the energy-efficient NCS.

A. SETUP

The experiments were performed to confirm the effectiveness of the MCDOB in the energy-efficient networked motion control system. Figure 10 shows the experimental setup, which includes a DC motor and controller. The motor control system was programmed under LabVIEW environment. The network delays and sleep-based energy-efficient network interfaces were emulated in the controller. The parameters were set as shown in Table 1. The relation between the proportional gain, K_p, and derivative gain, K_d, was determined so that the unit step response could be critical damping when the network interfaces were always active. The thresholds for the forward and feedback paths, h_1 and h_2, were set so that the ISE and communication rate were as small as possible. The ISE was calculated as (20)

$$ISE = \sum_{k=0}^{k_{end}} \left(\theta^{cmd}(k) - \theta^{res}(k)\right)^2 t_c, \tag{20}$$

where k_{end} was set to 5000 because the whole experimental period and control period were set to 5 s and 0.001 s, respectively.

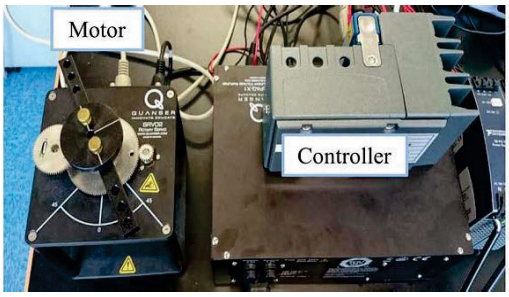

FIGURE 10. Experimental setup.

TABLE 1. Experimental parameters.

Nominal steady-state gain of the motor	K_n	1.53
Nominal time constant of the motor	τ_n	0.0254
Proportional gain	K_p	225
Derivative gain	K_d	30
Cut-off frequency of the DOB	g_{dob}	200 rad/s
Cut-off frequency of the MCDOB	g_{cdob}	200 rad/s
Voltage threshold for the forward path	h_1	0.01 V
Angle threshold for the feedback path	h_2	0.01 rad
Control period	t_c	0.001 s

In the experiments, an angle step command of 1 rad was input at 1 s. The effectiveness of the proposed method was evaluated in terms of the ISE and communication rate when the network delays, T_1 and T_2, and sleep periods, T_{s1} and T_{s2}, were changed. The communication rate was defined as the time occupancy of active mode for each transmitter, which indicates the power consumption of the transmitter. The controller with MCDOB needs more memory compared to the controller without MCDOB because the nominal model of the motor system and the low-pass filter have integrators. However, the controller worked with the control period of 1 ms and the increase in computational complexity did not affect the control performance in the experiments.

B. RESULTS

The experiments were performed for the following three cases; $T_{s1} = T_{s2} = 10$ ms, 20 ms, or 50 ms. It has been reported that the wake-up time of an optical transceiver is from 2 ms to 5 ms, and the power-saving effect is saturated when the sleep period approaches 50 ms [17]. Therefore, the sleep periods of the transmitters were set in the range between 10 ms and 50 ms.

The experimental results of the ISE and the communication rate when the sleep periods, T_{s1} and T_{s2}, were set to 10 ms for each network delay ($T_1 = T_2$) are shown in Figs. 11(a) and 11(b), respectively. From Fig. 11(a), in the system without MCDOB, the ISE increased by approximately 20 times more compared to the case with MCDOB at a 30-ms delay. From Fig. 11(b), the communication rate on the forward path

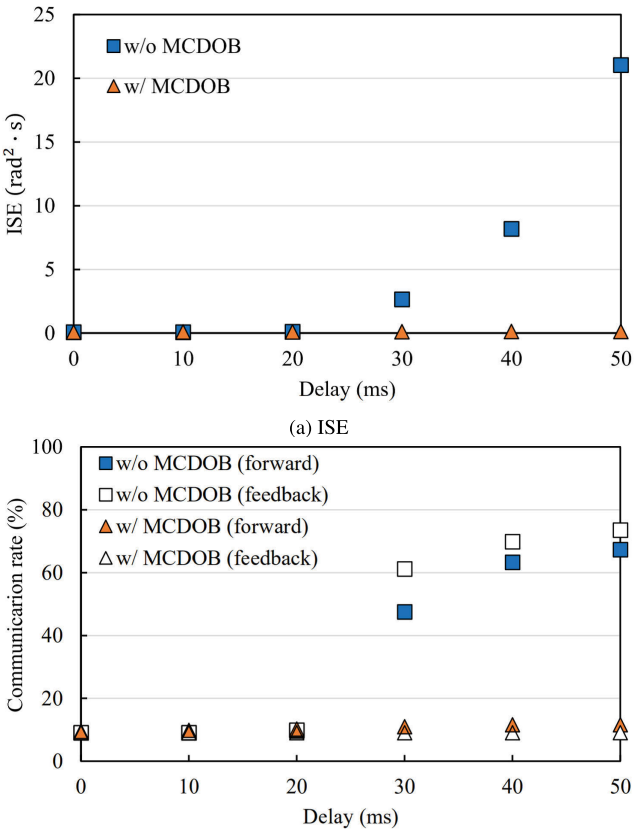

(a) ISE

(b) Communication rate

FIGURE 11. ISE and communication rate for each delay ($T_1 = T_2$, $T_{s1} = T_{s2} = 10$ ms).

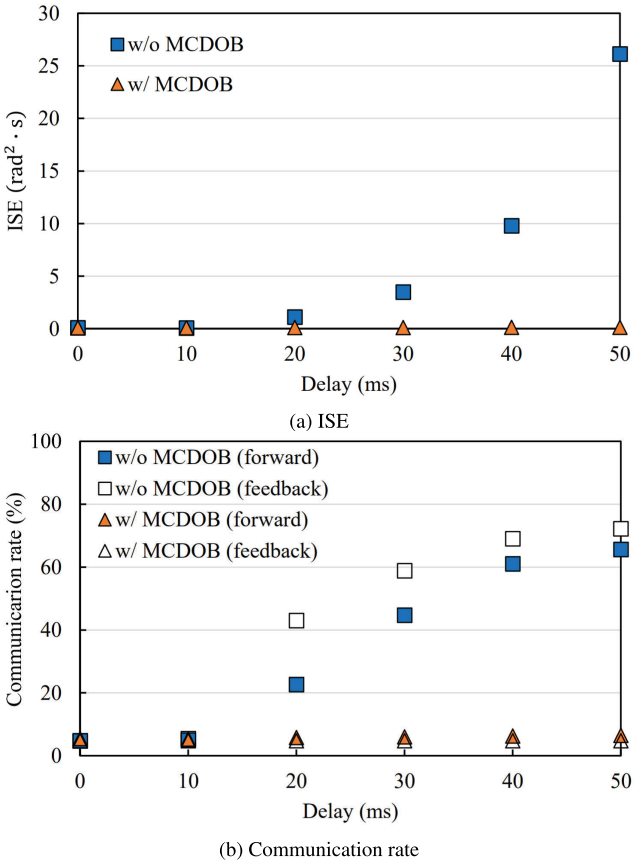

FIGURE 12. ISE and communication rate for each delay ($T_1 = T_2$, $T_{s1} = T_{s2} = 20$ ms).

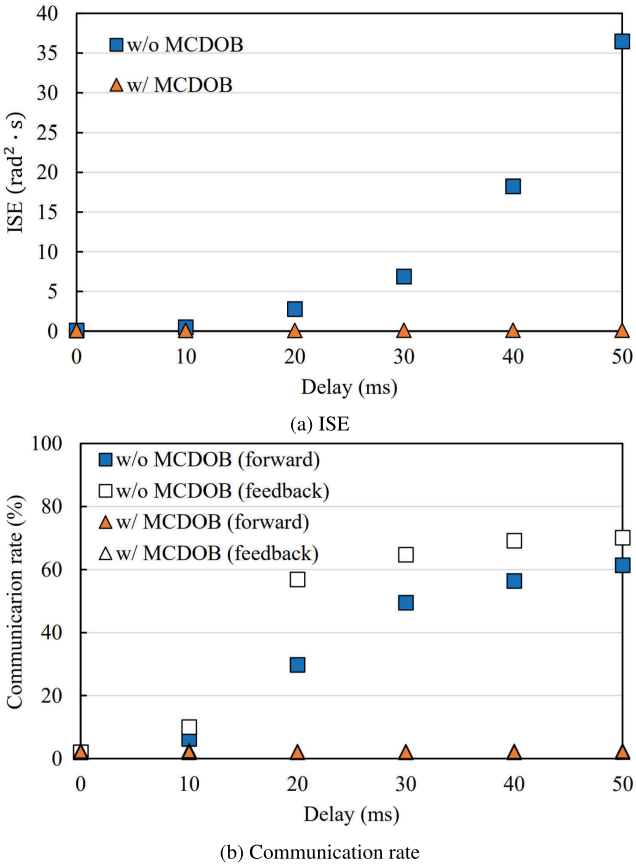

FIGURE 13. ISE and communication rate for each delay ($T_1 = T_2$, $T_{s1} = T_{s2} = 50$ ms).

increased by approximately 5 times more compared to the case with MCDOB at a 30-ms delay, while the communication rate on the feedback path increased by approximately 6 times more compared to the case with MCDOB at a 30-ms delay.

The experimental results of the ISE and the communication rate when the sleep periods, T_{s1} and T_{s2}, were set to 20 ms for each network delay ($T_1 = T_2$) are shown in Figs. 12(a) and 12(b), respectively. From Fig. 12(a), in the system without MCDOB, the ISE increased by approximately 10 times more compared to the case with MCDOB at a 20-ms delay. Fig. 12(b) shows that the communication rate on the forward path increased by approximately 4 times more compared to the case with MCDOB at a 20-ms delay, while the communication rate on the feedback path increased by approximately 10 times more compared to the case with MCDOB at a 20-ms delay.

The experimental results of the ISE and the communication rate when the sleep periods, T_{s1} and T_{s2}, were set to 50 ms for each network delay ($T_1 = T_2$) are shown in Figs. 13(a) and 13(b), respectively. From Fig. 13(a), in the system without MCDOB, the ISE increased by approximately 5 times more compared to the case with MCDOB at a 10-ms delay. From Fig. 13(b), the communication rate on the forward path increased by approximately 3 times more compared to the case with MCDOB at a 10-ms delay, while the communication rate on the feedback path increased approximately 5 times more compared to the case with MCDOB at a 10-ms delay.

From Fig. 11(a), 12(a), and 13(a), the ISE of the system without MCDOB became larger as the sleep periods became longer even if the delays were small because the system was affected by the sleep-induced data loss for a longer time. From Fig. 11(b), 12(b), and 13(b), the communication rate of the system without MCDOB became larger as the sleep periods became longer even if the delays were small because the increase in the data variation caused by oscillations prevented the transmitters from shifting to the sleep mode. In contrast, if the delays were enough small not to generate oscillations, the communication rates of the system without and with MCDOB became smaller as the sleep periods became longer because the transmitters were in the sleep mode for a longer time and more transmitted data decreased.

The step responses of the system without the MCDOB and with MCDOB are compared in Figs. 14(a) and 14(b), respectively. In the experiments, both network delays in the forward and feedback paths, T_1 and T_2, were set to 50 ms and the sleep periods, T_{s1} and T_{s2}, were set to 50 ms. From Fig. 14(a), in the

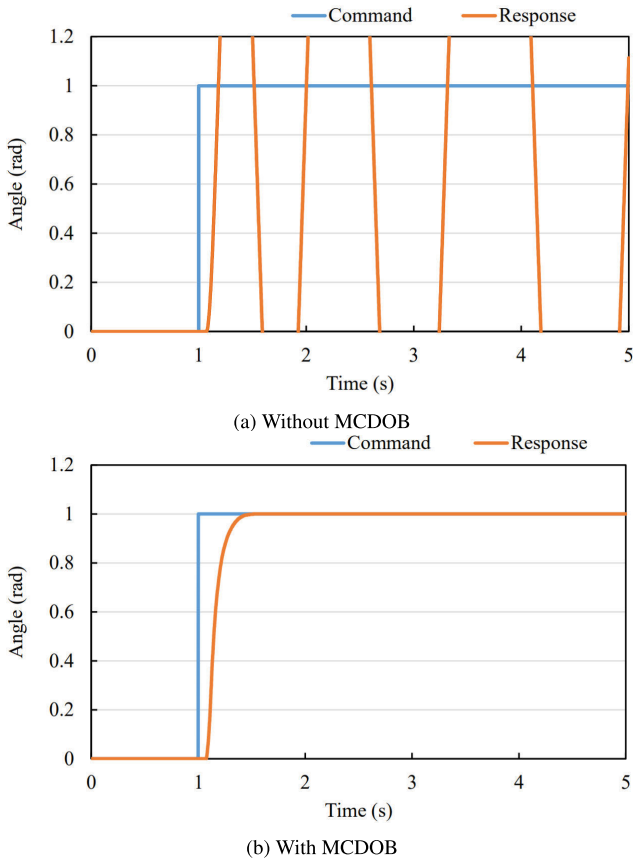

FIGURE 14. Step responses ($T_1 = T_2 = 50$ ms, $T_{s1} = T_{s2} = 50$ ms).

system without MCDOB, the step response provided a persistent oscillation and could not converge with the command. In contrast, from Fig. 14(b), in the system with MCDOB, the step response could converge with the command. The above results confirmed that the ISE and communication rate could be smaller regardless of the delays and sleep periods by introducing MCDOB into the energy-efficient NCS.

VI. CONCLUSION

This paper proposed a time-delay and data-loss compensation method using the MCDOB for NCSs with sleep-based energy-efficient interfaces. The MCDOB could compensate for not only the network delay but also for sleep-induced data loss as a disturbance. The experimental results showed that the proposed method with MCDOB outperformed the conventional method without MCDOB in terms of ISE and communication rate, which indicated the power consumption of network interfaces.

Our future works include an approach to cybersecurity issues in the NCS with sleep-based energy-efficient network interfaces. For example, a false data injection attack [41] may induce misjudgment of entering the sleep mode, which results in destabilization of the system. The relationship between a security mechanism and energy-efficiency is also an open issue [42]. The MCDOB has a potential to compensate for the effects of various kinds of sleep-induced and network-induced disturbances including cyberattacks.

REFERENCES

[1] A. Al-Fuqaha, M. Guizani, M. Mohammadi, M. Aledhari, and M. Ayyash, "Internet of Things: A survey on enabling technologies, protocols, and applications," *IEEE Commun. Surveys Tuts.*, vol. 17, no. 4, pp. 2347–2376, 4th Quart., 2015.
[2] R. A. Gupta and M.-Y. Chow, "Networked control system: Overview and research trends," *IEEE Trans. Ind. Electron.*, vol. 57, no. 7, pp. 2527–2535, Jul. 2010.
[3] J. P. Hespanha, P. Naghshtabrizi, and Y. Xu, "A survey of recent results in networked control systems," *Proc. IEEE*, vol. 95, no. 1, pp. 138–162, Jan. 2007.
[4] X.-M. Zhang, Q.-L. Han, X. Ge, D. Ding, L. Ding, D. Yue, and C. Peng, "Networked control systems: A survey of trends and techniques," *IEEE/CAA J. Automatica Sinica*, vol. 7, no. 1, pp. 1–17, Jan. 2020.
[5] T. Samad, J. S. Bay, and D. Godbole, "Network-centric systems for military operations in urban terrain: The role of UAVs," *Proc. IEEE*, vol. 95, no. 1, pp. 92–107, Jan. 2007.
[6] H. Laaki, Y. Miche, and K. Tammi, "Prototyping a digital twin for real time remote control over mobile networks: Application of remote surgery," *IEEE Access*, vol. 7, pp. 20325–20336, 2019.
[7] F. Blaabjerg, R. Teodorescu, M. Liserre, and A. V. Timbus, "Overview of control and grid synchronization for distributed power generation systems," *IEEE Trans. Ind. Electron.*, vol. 53, no. 5, pp. 1398–1409, Oct. 2006.
[8] T. Farjam, T. Charalambous, and H. Wymeersch, "A timer-based distributed channel access mechanism in networked control systems," *IEEE Trans. Circuits Syst. II, Exp. Briefs*, vol. 65, no. 5, pp. 652–656, May 2018.
[9] A. Rahnama, M. Xia, and P. J. Antsaklis, "Passivity-based design for event-triggered networked control systems," *IEEE Trans. Autom. Control*, vol. 63, no. 9, pp. 2755–2770, Sep. 2018.
[10] Y. Batmani, M. Davoodi, and N. Meskin, "Event-triggered suboptimal tracking controller design for a class of nonlinear discrete-time systems," *IEEE Trans. Ind. Electron.*, vol. 64, no. 10, pp. 8079–8087, Oct. 2017.
[11] S. Vitturi and F. Tramarin, "Energy efficient Ethernet for real-time industrial networks," *IEEE Trans. Autom. Sci. Eng.*, vol. 12, no. 1, pp. 228–237, Jan. 2015.
[12] Y. Sadi and S. Coleri Ergen, "Energy and delay constrained maximum adaptive schedule for wireless networked control systems," *IEEE Trans. Wireless Commun.*, vol. 14, no. 7, pp. 3738–3751, Jul. 2015.
[13] Y. Sadi and S. C. Ergen, "Joint optimization of wireless network energy consumption and control system performance in wireless networked control systems," *IEEE Trans. Wireless Commun.*, vol. 16, no. 4, pp. 2235–2248, Apr. 2017.
[14] R. Kubo, J.-I. Kani, Y. Fujimoto, N. Yoshimoto, and K. Kumozaki, "Adaptive power saving mechanism for 10 gigabit class PON systems," *IEICE Trans. Commun.*, vols. 93, no. 2, pp. 280–288, Feb. 2010.
[15] S.-W. Wong, L. Valcarenghi, S.-H. Yen, D. R. Campelo, S. Yamashita, and L. Kazovsky, "Sleep mode for energy saving PONs: Advantages and drawbacks," in *Proc. IEEE Globecom Workshops*, Nov. 2009, pp. 1–6.
[16] H. H. Lee, K.-O. Kim, J. H. Lee, and S. S. Lee, "Power saved OLT and ONU with cyclic sleep mode operating in WDM-PON," in *Proc. Int. Conf. ICT Converg. (ICTC)*, Oct. 2012, pp. 217–218.
[17] J. Mandin, "EPON power saving via sleep mode," presented at the IEEE 802.3av Task Force Meeting, Sep. 2008, pp. 15–33. [Online]. Available: http://www.ieee802.org/3/av/public/2008_09/index.html
[18] Y. Iino, T. Hatanaka, and M. Fujita, "Event-predictive control for energy saving of wireless networked control system," in *Proc. Amer. Control Conf.*, Jun. 2009, pp. 2236–2242.
[19] T. Funakoshi and R. Kubo, "Cyclic sleep control of network interfaces in feedback path for energy-efficient networked control systems," in *Proc. 2nd IEEJ Int. Workshop Sens., Actuation, Motion Control, Optim. (SAMCON)*, Mar. 2016, Paper V-6.
[20] L. Zhang, H. Gao, and O. Kaynak, "Network-induced constraints in networked control systems—A survey," *IEEE Trans. Ind. Informat.*, vol. 9, no. 1, pp. 403–416, Feb. 2013.
[21] Y. Zhang, S. Xie, L. Ren, and L. Zhang, "A new predictive sliding mode control approach for networked control systems with time delay and packet dropout," *IEEE Access*, vol. 7, pp. 134280–134292, 2019.
[22] X. Liang, J. Xu, and H. Zhang, "Optimal control and stabilization for networked control systems with packet dropout and input delay," *IEEE Trans. Circuits Syst. II, Exp. Briefs*, vol. 64, no. 9, pp. 1087–1091, Sep. 2017.

[23] R. Wang, G.-P. Liu, W. Wang, D. Rees, and Y.-B. Zhao, "H_∞ control for networked predictive control systems based on the switched Lyapunov function method," *IEEE Trans. Ind. Electron.*, vol. 57, no. 10, pp. 3565–3571, Oct. 2010.
[24] O. J. M. Smith, "A controller to overcome dead time," *Indian Sci. Assoc. Jpn.*, vol. 6, no. 2, pp. 28–33, 1959.
[25] C.-L. Lai and P.-L. Hsu, "Design the remote control system with the time-delay estimator and the adaptive smith predictor," *IEEE Trans. Ind. Informat.*, vol. 6, no. 1, pp. 73–80, Feb. 2010.
[26] M. Hamdy, S. Abd-Elhaleem, and M. A. Fkirin, "Adaptive fuzzy predictive controller for a class of networked nonlinear systems with time-varying delay," *IEEE Trans. Fuzzy Syst.*, vol. 26, no. 4, pp. 2135–2144, Aug. 2018.
[27] H. Xing, J. Ploeg, and H. Nijmeijer, "Smith predictor compensating for vehicle actuator delays in cooperative ACC systems," *IEEE Trans. Veh. Technol.*, vol. 68, no. 2, pp. 1106–1115, Feb. 2019.
[28] K. Natori and K. Ohnishi, "A design method of communication disturbance observer for time delay compensation," in *Proc. 32nd Annu. Conf. IEEE Ind. Electron. IECON*, Nov. 2006, pp. 730–735.
[29] W. Zhang, M. Tomizuka, P. Wu, Y.-H. Wei, Q. Leng, S. Han, and A. K. Mok, "A double disturbance observer design for compensation of unknown time delay in a wireless motion control system," *IEEE Trans. Control Syst. Technol.*, vol. 26, no. 2, pp. 675–683, Mar. 2018.
[30] R. Saito, K. Tsuchida, and T. Yokoyama, "Digital control of PWM inverter using ultra high speed network for feedback signals with communication disturbance observer based on rocket I/O protocol," in *Proc. Int. Power Electron. Conf. (IPEC-Hiroshima ECCE ASIA)*, May 2014, pp. 3397–3402.
[31] R. Imai and R. Kubo, "Experimental validation of communication disturbance observer for networked control systems with information losses," *IEICE Commun. Express*, vol. 5, no. 4, pp. 102–107, Apr. 2016.
[32] A. Onat, T. Naskali, E. Parlakay, and O. Mutluer, "Control over imperfect networks: Model-based predictive networked control systems," *IEEE Trans. Ind. Electron.*, vol. 58, no. 3, pp. 905–913, Mar. 2011.
[33] H. Li, M.-Y. Chow, and Z. Sun, "EDA-based speed control of a networked DC motor system with time delays and packet losses," *IEEE Trans. Ind. Electron.*, vol. 56, no. 5, pp. 1727–1735, May 2009.
[34] T. Ogura, K. Kobayashi, H. Okada, and M. Katayama, "H-infinity control design considering packet loss as a disturbance for networked control systems," *IEICE Trans. Fundamentals Electron., Commun. Comput. Sci.*, vol. 100, no. 2, pp. 353–360, Feb. 2017.
[35] T. Yamanaka, K. Yamada, R. Hotchi, and R. Kubo, "Time-delay and data-loss compensation using communication disturbance observer for energy-efficient networked control systems," in *Proc. Int. Symp. Nonlinear Theory Appl. (NOLTA)*, Dec. 2019, pp. 577–580.
[36] R. Imai and R. Kubo, "Introducing jitter buffers in networked control systems with communication disturbance observer under time-varying communication delays," in *Proc. 41st Annu. Conf. IEEE Ind. Electron. Soc. IECON*, Nov. 2015, pp. 2956–2961.
[37] K. Ohnishi, M. Shibata, and T. Murakami, "Motion control for advanced mechatronics," *IEEE/ASME Trans. Mechatronics*, vol. 1, no. 1, pp. 56–67, Mar. 1996.
[38] K. Natori and K. Ohnishi, "A design method of communication disturbance observer for time-delay compensation, taking the dynamic property of network disturbance into account," *IEEE Trans. Ind. Electron.*, vol. 55, no. 5, pp. 2152–2168, May 2008.
[39] K. Natori, R. Oboe, and K. Ohnishi, "Stability analysis and practical design procedure of time delayed control systems with communication disturbance observer," *IEEE Trans. Ind. Informat.*, vol. 4, no. 3, pp. 185–197, Aug. 2008.
[40] K. Natori, T. Tsuji, K. Ohnishi, A. Hace, and K. Jezernik, "Time-delay compensation by communication disturbance observer for bilateral teleoperation under time-varying delay," *IEEE Trans. Ind. Electron.*, vol. 57, no. 3, pp. 1050–1062, Mar. 2010.
[41] K. Yamada, J. Hoshino, and R. Kubo, "Detection of data tampering attacks using redundant network paths with different delays for networked control systems," *Nonlinear Theory Appl., IEICE*, vol. 10, no. 2, pp. 140–156, Apr. 2019.
[42] R. Muradore and D. Quaglia, "Energy-efficient intrusion detection and mitigation for networked control systems security," *IEEE Trans. Ind. Informat.*, vol. 11, no. 3, pp. 830–840, Jun. 2015.

TAKAHARU YAMANAKA received the B.E. degree in electronics and electrical engineering from Keio University, Japan, in 2019, where he is currently pursuing the M.E. degree in integrated design engineering. He is a Student Member of the Institute of Electronics, Information, and Communication Engineers (IEICE).

KENTA YAMADA received the B.E. degree in electronics and electrical engineering and the M.E. degree in integrated design engineering from Keio University, Japan, in 2017 and 2019, respectively.

RYOSUKE HOTCHI received the B.E. degree in electronics and electrical engineering and the M.E. degree in integrated design engineering from Keio University, Japan, in 2016 and 2018, respectively, where he is currently pursuing the Ph.D. degree in integrated design engineering. His research interests include network control and queue control systems.

He is a Student Member of the Institute of Electronics, Information, and Communication Engineers (IEICE).

RYOGO KUBO (Member, IEEE) received the B.E. degree in system design engineering and the M.E. and Ph.D. degrees in integrated design engineering from Keio University, Japan, in 2005, 2007, and 2009, respectively.

In 2007, he joined the NTT Access Network Service Systems Laboratories, NTT Corporation, Japan. Since 2010, he has been with Keio University, Japan, where he is currently an Associate Professor with the Department of Electronics and Electrical Engineering. From 2019 to 2020, he also held the position of Honorary Research Fellow at the Department of Electronic and Electrical Engineering, University College London (UCL), U.K. His research interests include system control, optical communications, networking, and cyber-physical systems. He is a member of the Optical Society (OSA), the Institute of Electrical Engineers of Japan (IEEJ), the Institute of Electronics, Information and Communication Engineers (IEICE), and the Society of Instrument and Control Engineers (SICE). He received the Best Paper Award from the IEICE Communications Society, in 2011, the IEEE International Conference on Communications (ICC '12) Best Paper Award, in 2012, the Leonard G. Abraham Prize from the IEEE Communications Society, in 2013, and the 2018 IEEE International Conference on Intelligence and Safety for Robotics (ISR '18) Best Paper Award, in 2018.